

Article

Feasibility of Different Methods for Separating *n*-Hexane and Ethanol

Aleksandra Sander , Ana Petračić , Marko Rogošić , Mirela Župan, Leonarda Frljak and Matija Cvetnić 

Faculty of Chemical Engineering and Technology, University of Zagreb, Trg Marka Marulića 19, 10000 Zagreb, Croatia; mrogosic@fkit.unizg.hr (M.R.); mima.zupan@gmail.com (M.Ž.); lfrljak@fkit.unizg.hr (L.F.); mcvetnic@fkit.unizg.hr (M.C.)

* Correspondence: asander@fkit.unizg.hr (A.S.); apetracic@fkit.unizg.hr (A.P.)

Abstract: Conventional distillation methods cannot effectively separate the components of an azeotropic mixture since both phases have the same composition, thereby preventing further separation. Additional techniques such as pressure swing distillation or distillation with entrainers are often employed to overcome this limitation and achieve separation. The aim of this investigation was to select the most effective method for separating *n*-hexane and ethanol. The feasibility of three methods was analyzed: reduced pressure distillation, extractive distillation, and liquid–liquid extraction. The mutual solubility of *n*-hexane and prepared deep eutectic solvents (DESs) (nine hydrophilic: choline chloride with glycerol, ethylene glycol, or carboxylic acid (malic, citric, glycolic); tetramethylammonium chloride with glycolic acid; lactic acid with glycerol; K₂CO₃ with glycerol or ethylene glycol; two hydrophobic: menthol with decanoic or dodecanoic acid) was experimentally determined. Extraction experiments were conducted to test the solubility of DESs in the feed mixture. The effect of changing DES-to-feed mass ratio was further investigated with choline chloride–glycerol (1:2). The same DES and both hydrophobic DESs were able to increase the relative volatility and enhance the separation of ethanol and *n*-hexane. Based on the obtained results, extraction was selected as the most effective method for the separation of *n*-hexane and ethanol.

Keywords: azeotropes; deep eutectic solvents; extraction; extractive distillation; liquid–liquid equilibrium; reduced pressure distillation



Citation: Sander, A.; Petračić, A.; Rogošić, M.; Župan, M.; Frljak, L.; Cvetnić, M. Feasibility of Different Methods for Separating *n*-Hexane and Ethanol. *Separations* **2024**, *11*, 151. <https://doi.org/10.3390/separations11050151>

Academic Editor: Gavino Sanna

Received: 29 April 2024

Revised: 10 May 2024

Accepted: 13 May 2024

Published: 15 May 2024



Copyright: © 2024 by the authors. Licensee MDPI, Basel, Switzerland. This article is an open access article distributed under the terms and conditions of the Creative Commons Attribution (CC BY) license (<https://creativecommons.org/licenses/by/4.0/>).

1. Introduction

The separation of azeotropic mixtures remains a challenging task in chemical processing industries, often requiring advanced separation techniques to achieve efficient and cost-effective results. Among the myriad of separation processes, extractive distillation and liquid–liquid extraction stand out for their potential to separate complex mixtures such as *n*-hexane and ethanol. However, the environmental impact, energy consumption, and efficiency of these processes can be significantly enhanced by innovative solvents such as deep eutectic solvents and ionic liquids (ILs).

DESs, a class of fluids akin to ILs but more benign and cost-effective, have emerged as a powerful alternative to conventional solvents for extraction and separation processes [1]. DESs are in general composed of a mixture of a hydrogen bond acceptor (HBA) and a hydrogen bond donor (HBD), melting at a temperature much lower than either of the starting components. Their unique properties—such as low volatility, non-flammability, and high solvation potential—make them ideal for use in separation processes where environmental and safety concerns are paramount.

In the context of separating *n*-hexane and ethanol, the selection of an effective solvent system is critical. The traditional approach often employs volatile organic compounds that pose significant environmental and health risks. Alternatively, DESs can provide an effective solution by enhancing selectivity and reducing the energy requirements of the

separation process. Table 1 lists recent papers dealing with separating *n*-hexane and ethanol (and some similar systems) with DESs and ILs.

Table 1. Overview of the recent literature data on the topic of *n*-hexane–ethanol azeotrope separation with DESs and ILs.

System	Solvent	Performance Characteristics	Literature
<i>n</i> -hexane + ethanol	Choline chloride, benzylcholinium chloride and tetrabutylammonium chloride as HBA and levulinic acid as HBD; mole ratio of 1 HBA:2 HBD	Discussed azeotrope-breaking ability, distribution coefficients, and selectivities.	[2]
<i>n</i> -hexane + ethanol	Choline chloride + malic acid, malonic acid; Ratio: 1:1 and 1:1:1	Detailed distribution coefficients and selectivities; data fitted with NRTL model	[3]
<i>n</i> -hexane + ethanol	Choline chloride + levulinic acid (1:2); choline chloride + ethylene glycol (1:2); choline chloride + malonic acid (1:1)	Detailed distribution coefficients and selectivities; data predicted by COSMO-SAC model	[4]
<i>n</i> -heptane + ethanol	Choline chloride + glycerol, levulinic acid, ethylene glycol; Choline chloride: HBD (1:2)	High selectivities and distribution coefficients compared to traditional solvents.	[1]
<i>n</i> -hexane/ <i>n</i> -heptane + ethanol	Choline chloride + 1,2-propanediol; Choline chloride: HBD (1:2)	Evaluated effect of water addition on extraction ability, enhancing understanding of DES performance.	[5]
<i>n</i> -hexane + ethanol	Hexyl(2-hydroxyethyl)dimethylammonium tetrafluoroborate or a hyperbranched polymer	High selectivity for separation of ethanol and hexane with the ammonium ionic liquid; data fitted with NRTL model	[6]
<i>n</i> -hexane + ethanol/ 1-propanol	[HMIM][BF ₄] and [HMIM][OTf]	Evaluated separation performance, distribution coefficients, and selectivity; data fitted with NRTL, UNIQUAC and UNIFAC models	[7]
<i>n</i> -hexane/ <i>n</i> -heptane + ethanol	Choline chloride + glycolic acid (1:1); choline chloride + lactic acid (1:2)	High selectivities and distribution coefficients; data fitted with NRTL model	[8]
<i>n</i> -hexane + ethanol	Choline chloride + oxalic acid or malonic acid; Choline chloride: HBD (1:1)	High selectivities and distribution coefficients; data fitted with NRTL model	[9]
<i>n</i> -hexane + ethanol	Phosphoric-based ionic liquids	High selectivities and distribution coefficients; data fitted with NRTL model	[10]

Oliveira et al. demonstrated that DESs based on choline chloride effectively separated azeotropic mixtures of *n*-heptane and ethanol, showing superior performance over traditional solvents in terms of selectivity and distribution coefficients, thereby reducing energy consumption in the overall process [1].

Similarly, Domanska et al. explored the use of an ionic liquid and a hyperbranched polymer for the liquid–liquid extraction of ethanol and *n*-hexane. Their findings indicated high selectivity in the separation using the ammonium ionic liquid, which could be correlated with experimental tie-lines using the Nonrandom Two-Liquid (NRTL) model. These studies underscore the potential of both ILs and DESs in replacing more hazardous solvents traditionally used in industrial separations [6].

The efficacy of DESs in these applications can be attributed to their ability to disrupt azeotropic compositions by altering the relative volatilities of the components in the mixture. This capability is crucial for breaking down complex mixtures that are otherwise challenging to separate due to their close boiling points or azeotropic behaviour. Studies by Gouveia et al. and Sharepour et al. further elaborate on the mechanisms by which DESs achieve this, emphasizing their role in enhancing the liquid–liquid equilibria and facilitating the selective extraction of ethanol from *n*-hexane [2,3].

While DESs offer considerable advantages, the selection of the appropriate solvent system remains a nuanced decision influenced by multiple factors including solvent recovery, toxicity, and operational costs. Medina-Herrera et al. provided a comprehensive framework for solvent selection in extractive distillation systems, which could be adapted to the selection of DESs in similar applications. This approach evaluates solvents based on their environmental impact, safety profiles, and economic feasibility, ensuring that the chosen solvents align with sustainability objectives and process efficiency [11].

Furthermore, the study of phase behaviour in systems involving DESs is critical for understanding the fundamental interactions and predicting the behaviour of these solvents in real-world applications. Research by Chen et al. offers insights into the phase behaviour and extraction mechanisms of ethanol–*n*-heptane systems using choline-based DESs, highlighting the complex intermolecular interactions that govern phase separations [12].

Incorporating advanced thermodynamic models such as NRTL and Universal Quasi-chemical Model (UNIQUAC) in the analysis of these systems further enhances the predictive capabilities and understanding of DES-based separations. These models help in interpreting the thermodynamic properties and interactions at the molecular level, providing a more robust theoretical foundation for the design and optimization of separation processes.

In conclusion, the integration of deep eutectic solvents into the separation of *n*-hexane and ethanol represents a significant advancement in the field of chemical engineering. By leveraging the unique properties of DESs, researchers and industry practitioners can achieve more efficient, safer, and environmentally friendly separations. Continued research and development in this area are essential for optimizing these processes, expanding the range of applications, and fully realizing the potential of deep eutectic solvents in industrial separations.

This research focuses on the separation of the *n*-hexane–ethanol mixture with both hydrophilic and hydrophobic DESs, via liquid–liquid extraction and extractive distillation. Reduced pressure distillation is conducted as well to compare how well it performs against extractive distillation in order to find the optimal process for this azeotropic separation.

2. Materials and Methods

Feed solution for all tested methods was composed of 65% (by weight) *n*-hexane and 35% absolute ethanol.

2.1. Chemicals

Chemicals used in this work are listed in Table 2. *n*-hexane, ethanol, menthol, decanoic, and dodecanoic acid were used without purification. Chemicals used for preparation of deep eutectic solvents were dried at reduced pressure ($p = 25$ mbar, $T = 60$ °C, $t = 8$ h). Hydrophilic DESs were prepared as described in the literature [13]. Hydrophobic DESs (menthol with decanoic or dodecanoic acid) were prepared by simple mixing of components at room temperature until clear liquid is obtained.

Table 2. List of chemicals.

Chemical	Manufacturer	CAS Number
<i>n</i> -hexane, p.a.	Carlo Erba	110-54-3
Ethanol absolute, p.a.	Alkaloid Skopje	64-17-5
Choline chloride, 99%	Acros Organics	67-48-1
Ethylene glycol, p.a.	Lach-Ner	107-21-1
Glycerol anhydrous	Lach-Ner	56-81-5
DL-Menthol, >98%	Thermo Scientific	89-78-1
Potassium carbonate, p.a.	Lach-Ner	584-08-7
Tetramethylammonium chloride, >98%	Thermo Scientific	75-57-0
Citric Acid monohydrate, p.a.	TTT	5949-29-1

Table 2. *Cont.*

Chemical	Manufacturer	CAS Number
L(+)-Lactic Acid, 80%	Lach-Ner	79-33-4
Glycolic Acid, >98%	TCI	79-14-1
DL-Malic Acid, >99%	Acros Organics	6915-15-7
Decanoic Acid, >98%	TCI	334-48-5
Dodecanoic Acid, >98%	TCI	143-07-7

Prepared DESs are listed in Table 3. Nine hydrophilic and two hydrophobic DESs were prepared for screening the appropriate solvent for a given method. A certain amount of water was added to DES 3, DES 4, and DES 6 to reduce their viscosity.

Table 3. List of the prepared DESs.

DES Type	Label	DES	Water, wt. %
Hydrophilic DESs	DES 1	ChCl-EG (1:2.5)	-
	DES 2	ChCl-Gly (1:2)	-
	DES 3	ChCl-CA (2:1)	30
	DES 4	ChCl-MA (1:1)	30
	DES 5	ChCl-GA (1:3)	-
	DES 6	LA-Gly (2:1)	10
	DES 7	K ₂ CO ₃ -Gly (1:6)	-
	DES 8	K ₂ CO ₃ -EG (1:10)	-
	DES 9	TMAC-GA (1:3)	-
Hydrophobic DESs	DES 10	M-DA (2:1)	-
	DES 11	M-DDA (2:1)	-

ChCl—choline chloride; EG—ethylene glycol; Gly—glycerol; CA—citric acid; MA—malic acid; GA—glycolic acid; LA—lactic acid; TMAC—tetramethylammonium chloride; M—menthol; DA—decanoic acid; DDA—dodecanoic acid.

2.2. Characterization of DESs and *n*-Hexane–Ethanol Mixtures

Density and surface tension (Wilhelmy plate method) were measured by DataPhysics tensiometer DCAT 8T. Viscosities of highly viscous DESs were measured using a Brookfield DV-III Ultra Programmable Rheometer (Spindle LV62). Viscosities of all other DESs were determined by a Cannon Fenske capillary viscometer (type 511 01). Mass fractions of *n*-hexane in binary mixtures with ethanol were determined by measuring the refractive index (Carl Zeiss Abbe refractometer, Jena, Germany). All physical properties were measured at 25 °C.

Concentrations of compounds in ternary mixtures were determined with a Shimadzu GC 2010 apparatus (Kyoto, Japan) equipped with a flame ionization detector (FID). The injection mode was headspace injection (HS). *N,N*-dimethylformamide (DMF, Supelco (Bellefonte, PA, USA), for headspace gas chromatography SupraSolv[®]) was used as co-solvent for headspace analysis. Approximately, 5 g DMF was added to approximately 50 mg of the standards and samples. The operating parameters for the headspace method were oven heating to 60 °C with shaking for 20 min. The headspace syringe was heated to 100 °C with a transfer temperature of 150 °C. A DB-624 column (3 µm film thickness, 30 m length, 0.53 mm inner diameter) was used for chromatographic separation. The analysis was performed isocratically at 40 °C for 20 min with N₂ as carrier gas and a flow rate of 5 mL/min. The FID detector was set to 240 °C with 30 and 400 mL/min H₂ and air, respectively.

Fourier-transform infrared spectroscopy (FTIR) and nuclear magnetic resonance spectroscopy (NMR) analyses were conducted on a Bruker Vertex 70 spectrometer and Bruker Avance 300 NMR spectrometer, respectively, according to previously described procedures [14].

2.3. Solvent Screening

2.3.1. Mutual Solubility of DESs and *n*-Hexane

Mutual solubility of *n*-hexane and prepared DESs was determined gravimetrically. To check the solubility of DESs in *n*-hexane, about 1 g of *n*-hexane was added to a 10 mL flask and titrated with DESs dropwise until a heterogeneous system was obtained (cloudy emulsion). Solubilities of *n*-hexane in DESs were established in a similar manner. Concentrations of both compounds were calculated from the measured masses.

2.3.2. Initial Extraction Experiments

Initial extraction experiments were performed to test the solubility of DESs in the feed mixture. All prepared DESs were mixed with the feed solution at 1:1 DES-to-feed mass ratio and agitated (250 rpm) for 12 h at room temperature. Raffinate and extract phases were separated after settling and refractive indices of raffinate were measured.

2.4. Reduced Pressure and Extractive Distillation

Distillation experiments were performed in a simple apparatus consisting of a round bottom flask ($V = 2 \text{ dm}^3$), heating mantle, column head with a valve stopcock acc. to Antilinger, an Erlenmeyer flask for collecting distillate, and two thermometers (for measuring vapor temperature at the entrance to the condenser and the bottom product). No distillation column was attached to the apparatus. Additionally, a vacuum pump was connected for experiments at reduced pressure. For extractive distillation experiments, an entrainer was added and mixed with the feed solution before heating. Experiments were carried out at total reflux. During all experiments, the changes in both temperatures were observed. After the stabilization of temperatures, samples of both phases were withdrawn to determine compositions, except for the extractive distillation, where only distillate composition was determined (samples without entrainer). Thus, the results presented correspond to batch distillation with total reflux operating in the stationary state, with at least two equilibrium stages involved. After initial screening of DESs, DES 2, DES 10, and DES 11 were selected as entrainers for extractive distillation ($p = 1 \text{ bar}$). Reduced pressure distillation was conducted at 0.2, 0.4, and 0.7 bar.

2.5. Liquid–Liquid Equilibrium

Solubility curve was determined experimentally by the cloud point method. Tie line compositions were obtained by a previously published procedure [15]. Raffinate composition was calculated from the calibration curve, $x = f(n_{D,25})$, while the composition of extract was obtained from the mass balance. Liquid–liquid equilibrium was correlated with NRTL and UNIQUAC models.

2.6. Extraction

The influence of DES-to-feed mass ratio was analyzed for the system *n*-hexane–ethanol–DES 2. Extraction experiments were performed in a laboratory batch extractor at the following process conditions: $T = 25 \text{ }^\circ\text{C}$, DES-to-feed mass ratios: 0.25, 0.5, 0.75, and 1, $n = 400 \text{ rpm}$ and $t = 2 \text{ h}$. Concentration of *n*-hexane in raffinate was measured after separation of phases.

2.7. Regeneration

After extraction, the phases were collected and evaporated on the rotary evaporator at $T = 60 \text{ }^\circ\text{C}$ and $p < 10 \text{ mbar}$ to remove all *n*-hexane and ethanol from DES 2. The dried DES was then analyzed using NMR spectroscopy.

3. Results and Discussion

Eleven DESs were prepared, characterized, and screened as selective solvents for extractive separation of azeotropic mixture ethanol–*n*-hexane. Three chosen DESs (DES 2,

DES 10, and DES 11) were also evaluated as entrainers for extractive distillation. Reduced pressure distillation was conducted as well, for comparison.

3.1. Physical Properties of DESs

Measured densities, viscosities, and surface tensions of the prepared DESs are presented in Table 4. All properties were determined at $T = 25\text{ }^{\circ}\text{C}$.

Table 4. Physical properties of the prepared DESs.

DES	ρ , kg m^{-3}	η , mPa s	σ , mN m^{-1}
DES 1	1117.32	34.47	46.18
DES 2	1189.60	345.61	65.52
DES 3	1150.55	15.76	50.28
DES 4	1186.56	16.10	41.18
DES 5	1263.55	226.48	56.85
DES 6	1188.80	29.60	47.21
DES 7	1117.32	19,161.15	61.97
DES 8	1256.82	131.73	43.43
DES 9	1233.90	278.79	57.75
DES 10	896.35	20.89	23.31
DES 11	893.90	24.71	27.65

The physical properties of DESs, such as viscosity, density, and surface tension, play critical roles in determining their applicability and effectiveness in various industrial processes. Viscosity influences how easily a DES can be pumped and mixed in laboratory or industrial settings, impacting mass transfer rates and the efficiency of reactions and separations. Lower viscosities are generally preferred for processes where rapid mixing and heat transfer are needed. Density affects the separation characteristics of DESs, particularly in processes involving liquid–liquid extraction where differences in density are exploited to separate phases. Surface tension, on the other hand, plays a critical role in the effectiveness of solvents during extraction processes. Lower surface tension can enhance interfacial interactions between the DES and other liquids, facilitating better mixing and emulsification, which are important for efficient mass transfer. This improved mixing increases the contact area in liquid–liquid extractions, boosting the extraction efficiency.

Observing the data in Table 4, hydrophobic DESs exhibit lower densities, viscosities, and surface tensions when compared to hydrophilic DESs.

3.2. Solvent Screening

In order to find a suitable solvent for the azeotrope separation, DESs were mixed with *n*-hexane and the feed mixture containing 65% *n*-hexane and 35% ethanol to determine their mutual solubility and their possible application in liquid–liquid extraction and extractive distillation. This particular feed composition was chosen to enable a meaningful study of the influence of DES-to-feed mass ratio on the separation efficiency of extraction in the ternary heterogeneous system. The choice of a composition closer to the azeotropic point ($w = 78.03\%$ and $58.7\text{ }^{\circ}\text{C}$, at $p = 1\text{ bar}$) would produce too small differences in product concentrations. To make all the methods comparable, the same feed composition was used for other separation methods as well.

3.2.1. Mutual Solubility of *n*-Hexane and DESs

The mutual solubility of *n*-hexane and DES was determined gravimetrically. DES 1 and DES 6 turned out to be sparsely soluble in *n*-hexane, where 6.73% and 2.41% of DES were dissolved in *n*-hexane, respectively. DES 10 and DES 11 were completely miscible with *n*-hexane. When adding *n*-hexane to DES dropwise, DES 1, DES 2, and DES 8 dissolved 1.19%, 0.21%, and 0.44% of *n*-hexane. It is worth mentioning that the dissolution of *n*-hexane in more viscous DESs was hard to observe visually due to the large difference in viscosities

between *n*-hexane and DESs since experiments were performed at room temperature (to exploit one of the most important advantages of liquid–liquid extraction over distillation: performing separations at room temperature and atmospheric pressure). For that reason, the solubility of DESs in the feed mixture was further examined.

3.2.2. Solubility of DESs in the Feed Mixture

The solubility of DESs in the feed mixture was determined by mixing equal amounts of DES and feed mixture and agitating the mixtures for 12 h at 25 °C. DES 10 and DES 11 were found to be completely miscible with the feed mixture and a homogenous solution was obtained. This proved that those two DESs cannot be used for liquid–liquid extraction. The formation of a homogeneous mixture was expected. Ethanol can be dissolved in both polar and non-polar solvents, while *n*-hexane, as a highly non-polar solvent, can only be dissolved in non-polar hydrophobic solvents. The addition of all hydrophilic DESs resulted in the formation of two phases, so those solvents were further analyzed to determine if they could be used for extraction. Refractive indices of the raffinate samples were measured and for DES 1, DES 5, DES 6, DES 8, and DES 9 they turned out to be larger than for pure *n*-hexane, which indicated slight solubility of the tested DESs in the raffinate and eliminated those DESs from further considerations. Mass fractions of *n*-hexane in the raffinate, after mixing with the other four DESs, DES 2, DES 3, DES 4, and DES 7, were 0.975, 0.993, 0.997, and 0.837, respectively. The same four raffinate samples were then dried to determine the amount of DES possibly dissolved, but only DES 7 had 1.69% DES left on the plate after drying. DES 3 and DES 4 were eliminated from further research since they exhibited very low pH values and could as such be highly corrosive in an industrial environment. DES 7 exhibited a very high pH value and viscosity and was also found to be partially miscible with the feed mixture, so further extraction experiments were conducted with DES 2 only.

The miscibility of the DESs and feed mixture was also determined with FTIR spectroscopy and the FTIR spectra of selected DESs are given in Figure 1. To further investigate the solubility of DES 2, DES 3 and DES 4 in the raffinate phase, FTIR spectra of feed, raffinate phase, and DESs were recorded in Figure 1a–c. The absorption bands of ethanol (1091.08, 1049.62, and 880.87 cm^{-1}) showed a significant decrease in intensity, indicating the extraction of ethanol. FTIR results confirmed that DES 2 is insoluble in the raffinate phase, making it suitable for separating *n*-hexane and ethanol. In the fingerprint region of the raffinate phases after extraction with DES 3 and DES 4, absorption bands characteristic of the respective DESs could be observed [16]. Specifically, a peak around 950 cm^{-1} could be attributed to the C-N group of choline chloride, while another peak around 1250 cm^{-1} indicated C-O and C-N stretching, commonly found in amine-related structures like choline chloride [17]. Additionally, the FTIR spectrum of the raffinate treated with DES 4 showed an absorption band at 2981 cm^{-1} attributed to the CH_3 stretching of DES. The solubility of DES 3 and DES 4 in the raffinate could be attributed to the formation of stronger hydrogen bonds between ethanol and DESs in the presence of *n*-hexane compared to pure ethanol and DESs [18]. The molecules of ethanol and *n*-hexane in the feed solution tend to associate with molecules of the same type, driven by the formation of hydrogen bonds among ethanol molecules, leading to the creation of cyclic ethanol clusters [19]. Due to the stronger hydrogen bonds with DESs and the higher diffusion rate of ethanol in its mixture with *n*-hexane (which exhibits significantly weaker bonds between ethanol and *n*-hexane), ethanol can be easily separated using hydrophilic DESs as a selective solvent [20].

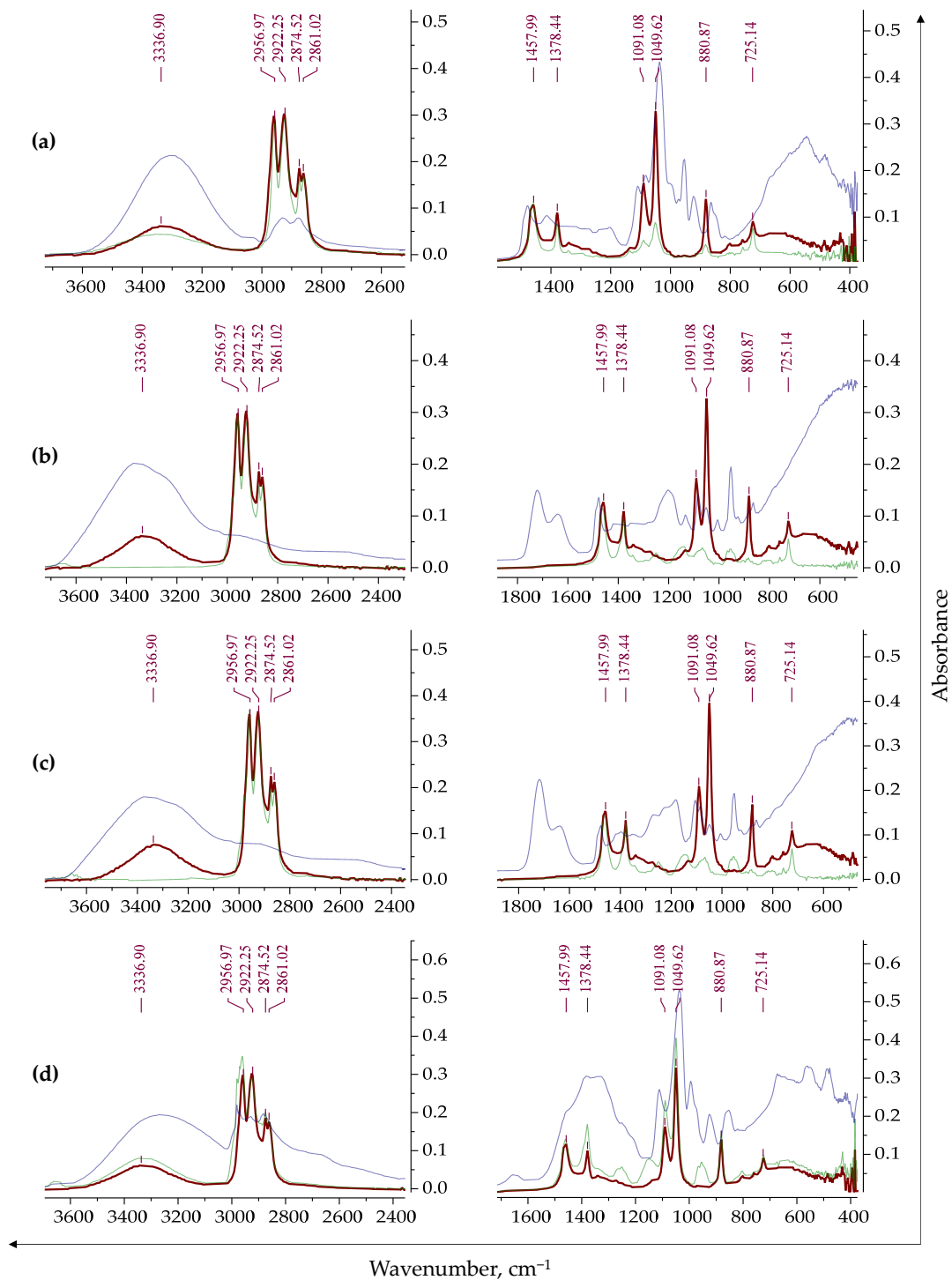


Figure 1. Enlarged FTIR spectra of feed (red), raffinate (green), and DES (blue): (a) DES 2; (b) DES 3; (c) DES 4; (d) DES 7.

As mentioned before, gravimetric tests had confirmed the partial solubility of DES 7 in the feed solution. However, upon analyzing the FTIR spectrum of DES 7, feed, and raffinate after mixing, no significant change could be observed in the raffinate besides the evolution of peaks that correspond to DES 7, Figure 1d. Extraction did not occur, as evidenced by the similar intensity of absorption bands of *n*-hexane and ethanol compared to those in the feed solution.

3.3. Reduced Pressure Distillation and Extractive Distillation

Extractive distillation was conducted with two hydrophobic DESs and with hydrophilic DES 2. The formation of a homogeneous system when the feed mixture was contacted with the two hydrophobic DESs makes those solvents excellent candidates for use as entrainers in extractive distillation. The hydrophilic DES was chosen in contrast to the two hydrophobic DESs, with higher viscosity and higher surface tension than DES 10 and DES 11. Even though the solvent used for extractive distillation should be completely miscible with the feed solution, DES 2 was chosen due to the observed good solubility of ethanol in it. Based on the results presented in Table 5, the addition of 5% hydrophilic DES 2 slightly increased the content of *n*-hexane in the distillate compared to the regular atmospheric distillation, and the addition of 10% DES2 resulted in a further slight increase. At the same time, the homogeneous system was converted to the heterogeneous one; however, this did not affect the vapor phase composition significantly. As DES 2 was supposed to affect the interaction of ethanol and *n*-hexane primarily through ethanol clusters, and since ethanol clusters in its mixture with *n*-hexane are mostly disrupted at increased temperatures, DES 2 was not found to significantly affect the interaction of ethanol and *n*-hexane at boiling temperatures and thus exhibited low entraining efficiency [20]. Thus, hydrogen bonding was found not to be decisive at elevated temperatures. Reducing the pressure also improved the effectiveness of the separation, Table 6, in line with the decrease in temperature and increase of the strength of hydrogen bonding associated with it. On the other hand, the addition of 5% hydrophobic DESs resulted in the most noticeable increase of *n*-hexane content in the vapor phase. Since hydrogen bonding interactions are not expected to play a significant role at boiling temperatures, the finding has to be attributed to the subtle balance of polar and dispersion interactions in the complex system under investigation.

Table 5. Compositions of distillate and both products' temperatures after extractive distillation experiments.

Entrainer	w_{DES}	$T_D, ^\circ C$	w_D (<i>n</i> -Hexane)	$T_B, ^\circ C$
DES 2	0.05	58.1	0.7305	59.5
	0.10	57.5	0.7370	59.0
DES 10	0.05	56.5	0.8735	58.6
DES 11	0.05	56.5	0.8718	58.6

Table 6. Compositions of distillate and bottom product and temperatures of bottom product after reduced pressure experiments.

p, bar	w_B (<i>n</i> -Hexane)		$T_B, ^\circ C$		w_D (<i>n</i> -Hexane)
	Experimental	Experimental	UNIFAC	UNIFAC	Experimental
1	0.2491	62.5	62.7		0.7223
0.7	0.2525	53.0	53.2		0.7464
0.4	0.2548	40.0	39.5		0.7556
0.2	0.2289	23.0	24.9		0.7931

The experimental temperatures of the bottom product were compared with the UNIFAC predictions for given experimental bottom product compositions, using a literature set of parameters [21]. The agreement seems to be fair, in particular at higher pressures and temperatures in the range of validity of UNIFAC parameters.

3.4. Liquid–Liquid Equilibrium

Experimental data on liquid–liquid equilibrium are usually modeled using correlative activity coefficient models, for example, the NRTL [22] and UNIQUAC [23] models. The

NRTL model has three parameters per pair of components. The excess Gibbs energy is described by the expression:

$$\frac{g^{ex}}{RT} = \sum_{i=1}^{n_c} x_i \left[\frac{\sum_{j=1}^{n_c} \tau_{ji} G_{ji} x_j}{\sum_{k=1}^{n_c} G_{ki} x_k} \right], \tag{1}$$

with

$$G_{ij} = \exp(-\alpha_{ij} \tau_{ij}), \tag{2}$$

therein, $n_c = 3$ is the number of (quasi)components in the system, and x_i is the system composition in terms of molar fractions. The non-randomness parameter α_{ij} is rarely regressed; instead, its value is fixed empirically, in this case to 0.2. The remaining six interaction parameters τ_{ij} are determined by a suitable regression procedure.

The UNIQUAC model has a combinatorial and residual part. The combinatorial part is expressed by:

$$\frac{g^{ex,C}}{RT} = \sum_{i=1}^{n_c} x_i \ln \frac{\Phi_i}{x_i} + \frac{z}{2} \sum_{i=1}^{n_c} q_i x_i \ln \frac{\Theta_i}{\Phi_i}, \tag{3}$$

and describes the non-ideality of the solution as a consequence of the difference in the size and shape of the molecules of the (quasi)components. The surface fractions, Θ_i , and volume fractions, Φ_i , of the components are determined from the corresponding surface and volume parameters, shown in Table 7. For ethanol and *n*-hexane, they are calculated using tabulated literature data [24]. Regarding DES 2, it is considered a quasi-component in this case; this means that that it distributes between the two phases while maintaining its composition. Surface and volume parameters were estimated from experimentally determined densities by applying appropriate empirical correlations [6].

Table 7. Surface (r_i) and volume (q_i) parameters of UNIQUAC.

	r	q
DES 2	7.897	6.518
Ethanol	2.5755	2.588
<i>n</i> -Hexane	4.4998	3.856

The residual part is written as:

$$\frac{g^{ex,R}}{RT} = - \sum_{i=1}^{n_c} q_i x_i \ln \left(\sum_{j=1}^{n_c} \Theta_j \tau_{ji} \right). \tag{4}$$

The six interaction parameters τ_{ij} are regressed by a suitable procedure from the tie lines, as for the NRTL model.

In this work, the regression procedure was applied that was described in detail elsewhere [25]. In the first stage of the procedure, the minimum of the objective function derived from the equality of activity of the components in the equilibrium state is sought:

$$OF_1 = \sum_{j=1}^{n_d} \sum_{i=1}^{n_c} \left[\left(x_i^R \gamma_i^R - x_i^E \gamma_i^E \right) / \left(x_i^R \gamma_i^R + x_i^E \gamma_i^E \right) \right]_j^2 + Q \left(\tau_{12}^2 + \tau_{21}^2 + \tau_{13}^2 + \tau_{31}^2 + \tau_{23}^2 + \tau_{32}^2 \right). \tag{5}$$

In the second stage, the minimum of the following function is searched for:

$$OF_2 = \sum_{j=1}^{n_d} \sum_{i=1}^{n_c} \sum_{p=R,E} \left[\left(w_i^p \right)_{exp} - \left(w_i^p \right)_{mod} \right]_j^2 + Q \left(\tau_{12}^2 + \tau_{21}^2 + \tau_{13}^2 + \tau_{31}^2 + \tau_{23}^2 + \tau_{32}^2 \right), \tag{6}$$

where n_d indicates the number of tie lines determined, x_i and w_i stand for the molar and mass fractions of the components, γ_i are the activity coefficients of the components, R and E indicate the extract and raffinate phase, p denotes the phase in general, and the indices exp and mod refer to experimental data and model-calculated data. The procedure proved to be suitable for systems with large differences in molar masses of (quasi)components; the composition variable in the regression is mass fraction, but all internal calculations of excess Gibbs energies and activity coefficients are performed with molar fractions. Q is a penalty function with values $Q = 1 \times 10^{-6}$ for OF_1 and $Q = 1 \times 10^{-10}$ for OF_2 for both models; the values are selected from the literature [26].

The optimal interaction parameters of both models and values of the average absolute deviation of experimental and calculated mass fractions, according to

$$A = \sqrt{OF_2 - Q(\tau_{12}^2 + \tau_{21}^2 + \tau_{13}^2 + \tau_{31}^2 + \tau_{23}^2 + \tau_{32}^2) / (n_d \cdot 2 \times 3)} \tag{7}$$

are shown in Table 8.

Table 8. Optimal NRTL and UNIQUAC model parameters and average absolute prediction errors for the system *n*-hexane–ethanol–DES 2.

	τ_{12}	τ_{13}	τ_{21}	τ_{23}	τ_{31}	τ_{32}	A
NRTL	−0.3650	11.0701	2.2939	1.8427	9.0683	0.0632	0.0234
UNIQUAC	1.6654	0.1392	0.4348	1.3909	0.5903	0.4472	0.0039

The results show that both models describe the experimental data relatively well, with the values of the root mean square deviation of the composition favouring the UNIQUAC model. It should be noted here that the consistency of the model parameters was tested and approved by the procedure proposed by Marcilla et al. [27]. The experimental and model tie lines are compared in Table 9 and Figure 2.

Table 9. Tie lines data for the system *n*-hexane (1)—ethanol (2)—DES 2 (3) (mass fractions).

Raffinate								
experimental			NRTL			UNIQUAC		
w_1	w_2	w_3	w_1	w_2	w_3	w_1	w_2	w_3
0.9743	0.0256	0.0001	0.9474	0.0522	0.0003	0.9683	0.0314	0.0003
0.8900	0.1089	0.0011	0.8450	0.1523	0.0027	0.8899	0.1087	0.0014
0.7705	0.2235	0.0060	0.7311	0.2590	0.0099	0.7769	0.2169	0.0062
0.6669	0.3160	0.0171	0.6290	0.3486	0.0224	0.6560	0.3247	0.0193
0.4950	0.4544	0.0506	0.5002	0.4496	0.0502	0.4957	0.4489	0.0553
0.4029	0.5060	0.0911	0.4118	0.5075	0.0807	0.4078	0.5049	0.0873
Extract								
experimental			NRTL			UNIQUAC		
w_1	w_2	w_3	w_1	w_2	w_3	w_1	w_2	w_3
0	0.0760	0.9239	0.0002	0.0531	0.9467	0.0006	0.0712	0.9282
0	0.1939	0.8061	0.0035	0.1541	0.8425	0.0041	0.1937	0.8022
0.0175	0.2947	0.6878	0.0136	0.2616	0.7247	0.0137	0.3006	0.6857
0.0290	0.3822	0.5888	0.0296	0.3513	0.6192	0.0275	0.3749	0.5977
0.0500	0.4444	0.5056	0.0605	0.4489	0.4906	0.0520	0.4495	0.4986
0.0780	0.4866	0.4354	0.0795	0.4859	0.4347	0.0717	0.4876	0.4407

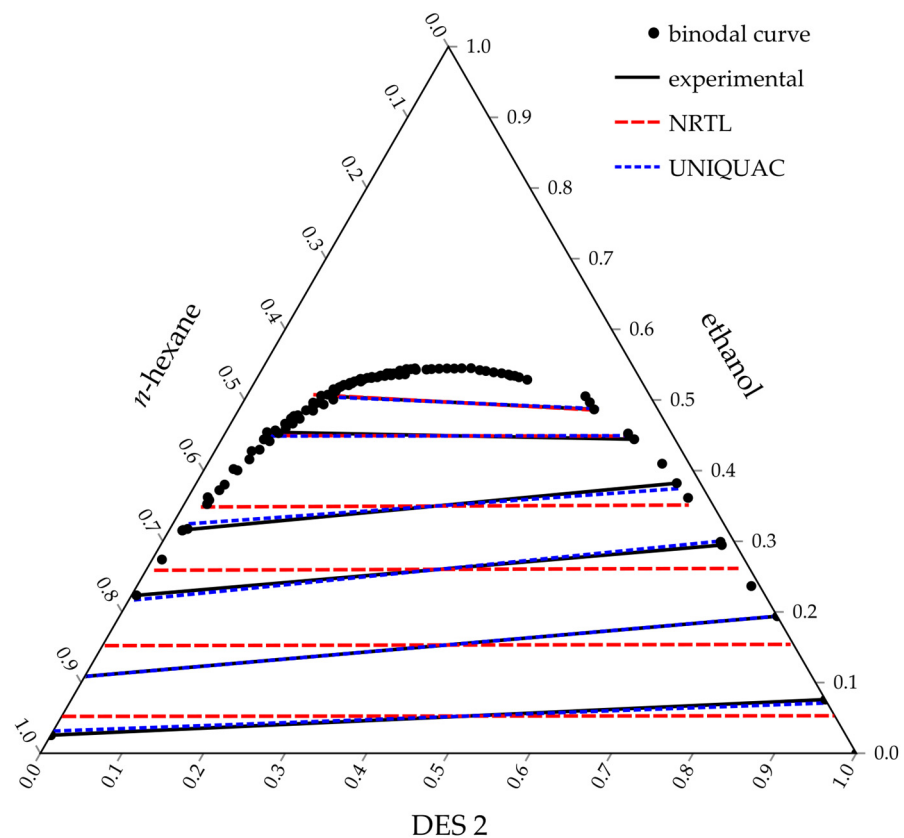


Figure 2. Binodal and tie line data for the system *n*-hexane (1)—ethanol (2)—DES 2 (3).

The ternary diagram of the system *n*-hexane (1)—ethanol (2)—DES 2 (3) is given in Figure 2. The system shows a large immiscible region, with *n*-hexane and DES 2 being almost completely immiscible. At lower ethanol concentration, the slope of the tie lines is positive, and their outline is perfectly traced with the UNIQUAC model. At higher ethanol concentrations, the slope becomes negative and both models accurately predict the last two tie lines.

Due to the absence of *n*-hexane in the extract phase for the first two experimental tie lines, it is impossible to calculate the distribution coefficient of *n*-hexane and therefore the selectivity, which makes it very hard to compare these results with literature since the authors usually compare their results at very low ethanol concentrations. Since selectivities in this work can be calculated only for the raffinate phases above 22% of ethanol from experimental data, the data obtained from the UNIQUAC model were also used to calculate distribution coefficients and selectivities. The calculated values for both experimental and fitted data are given in Table 10.

Table 10. Ethanol concentrations in the raffinate, distribution coefficients, and selectivities of DES 2.

Experimental				UNIQUAC			
w_2	$\beta_{n\text{-hexane}}$	β_{ethanol}	S	w_2	$\beta_{n\text{-hexane}}$	β_{ethanol}	S
0.0256	0	2.9696		0.0314	0.0006	2.2709	3831.43
0.1089	0	1.7811		0.1087	0.0046	1.7818	386.01
0.2235	0.0227	1.3186	58.05	0.2169	0.0176	1.3858	78.61
0.3160	0.0435	1.2096	27.82	0.3247	0.0419	1.1544	27.56
0.4544	0.1010	0.9780	9.68	0.4489	0.1048	1.0012	9.55
0.5060	0.1936	0.9617	4.97	0.5049	0.1758	0.9659	5.49

It is worth noting that temperature also affects the distribution coefficients and therefore selectivities, so it must be considered when comparing data with the literature. Samarov et al. conducted their experiments with *n*-hexane–ethanol and two choline chloride-based DESs (with oxalic and malonic acid; 1:1 molar ratio). They found that the increase in temperature from 293.15 K to 313.15 K resulted in an increase of selectivity for the DES with oxalic acid, but for the DES with malonic acid, the selectivity decreased. At the comparable ethanol contents of 3.7% and 3.5%, the selectivities for DES with oxalic acid were 1162 and 1683, at 293.15 and 313.15 K, respectively. For DES with malonic acid, the selectivities at comparable 3.1% and 2.6% of ethanol were 3405 and 1779 at 293.15 and 313.15 K, respectively [9]. Sa et al. conducted their experiments with choline chloride-based DESs and levulinic acid, ethylene glycol and malonic acid in molar ratios 1:2, 1:2, and 1:1, respectively, at 298.2 K. At the comparable ethanol concentrations of 1.7%, 2.3% and 3.9%, the selectivities of the abovementioned DESs are 684.6, 864.53 and 854.77, respectively. It is worth noting that for the DES with malonic acid, the selectivity at 2% ethanol is 6410.64 [4]. Sa et al. also used choline chloride-based DESs with 1,4-butanediol at 1:3, 1:4, and 1:5 molar ratios, respectively. Their selectivities at 3.11%, 3.43%, and 1.58% were 301.7, 541.94 and 1491.99 for the abovementioned DESs, respectively [28].

When comparing the data in Table 10 with the literature data, it can be concluded that DES 2 exhibits high selectivity and is a suitable solvent for the extraction of ethanol. Hydrogen bond interactions between the DES and the solvent, and polarity differences between DES and *n*-hexane play a significant role in the DESs success.

3.5. Extraction

The extraction experiments with DES 2 were conducted at different DES-to-feed mass ratios. It can be clearly seen that increasing the amount of DES results in better separation and larger extraction efficiencies, selectivity, and distribution coefficients for ethanol, which is observable in Figure 3. The initial feed composition was 65% *n*-hexane and 35% ethanol. Raffinate and extract compositions are given in Table 11.

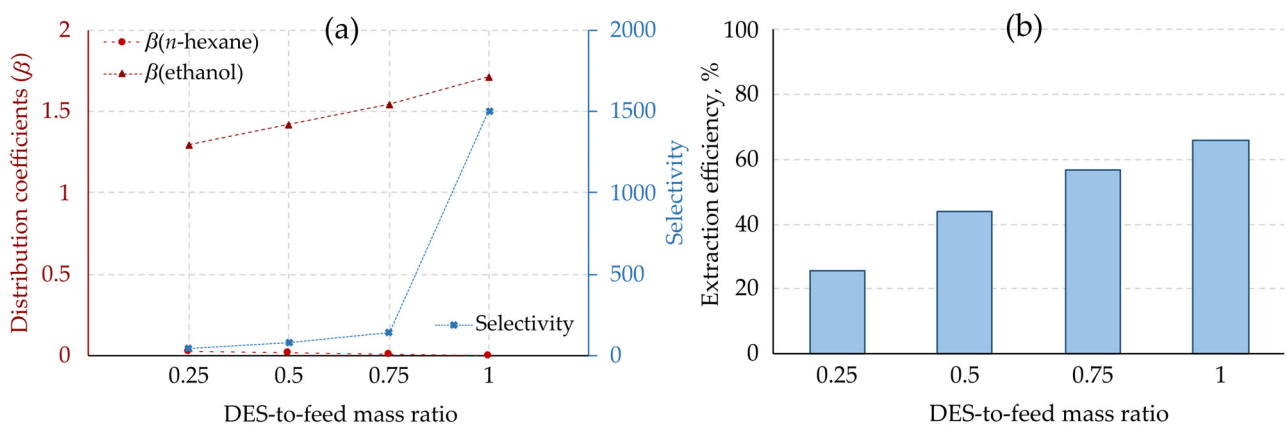


Figure 3. (a) Distribution coefficient and selectivity and (b) extraction efficiency at different DES-to-feed mass ratios.

Table 11. The influence of the DES-to-feed mass ratio on the compositions (mass fractions) of raffinate and extract for the system *n*-hexane (1)—ethanol (2)—DES 2 (3).

Mass Ratio	Raffinate			Extract		
	w_1	w_2	w_3	w_1	w_2	w_3
0.25	0.7399	0.2600	0.0001	0.0220	0.3370	0.6410
0.50	0.8029	0.1970	0.0001	0.0140	0.2800	0.7060
0.75	0.8460	0.1520	0.0019	0.0090	0.2350	0.7560
1.00	0.8788	0.1200	0.0012	0.0010	0.2060	0.7930

The addition of a larger amount of DES 2 enables the formation of a larger number of stronger hydrogen bonds, which in turn results in the dissolution of a higher amount of ethanol in DES 2.

The selectivity and distribution coefficients for ethanol increase with increasing DES-to-feed mass ratio, due to the larger affinity of DES 2 for ethanol than for nonpolar *n*-hexane.

3.6. Regeneration

After extraction, DES 2 was purified by means of vacuum evaporation. The obtained spectra are shown in Figure 4. The spectrum of DES 2 after extraction exhibits quite different signals than those of fresh and regenerated DES. On the enlarged parts of ^1H NMR spectrum of the extract phase (DES 2 after extraction) several signals can be observed: the hydroxyl proton of ethanol and/or glycerol at 4.72 ppm (due to strong hydrogen bonding or interactions with other compounds); the hydroxyl protons of $-\text{CH}_2\text{OH}$ groups in glycerol at 4.05 and 4.38 ppm (different chemical shifts than in DES 2 due to the different environment, which influences hydrogen bonding); peaks from 3.58 to 3.74 ppm can be related to the methylene group in ethanol (reflecting a different electronic environment); peaks from 3.41 to 3.33 ppm can be associated with the $\text{N}-(\text{CH}_3)_3$ group (shifted to the lower ppm due to the different environment than in pure DES); peak at 3.31 ppm can be attributed to methylene protons in ethanol; peaks from 0.80 to 1.33 ppm correspond to the methyl groups of *n*-hexane and ethanol. All peaks characteristic for *n*-hexane and ethanol visible on the ^1H NMR spectrum of DES 2 after extraction practically disappear after the purification step. This proves that DES 2 can easily be regenerated for further usage.

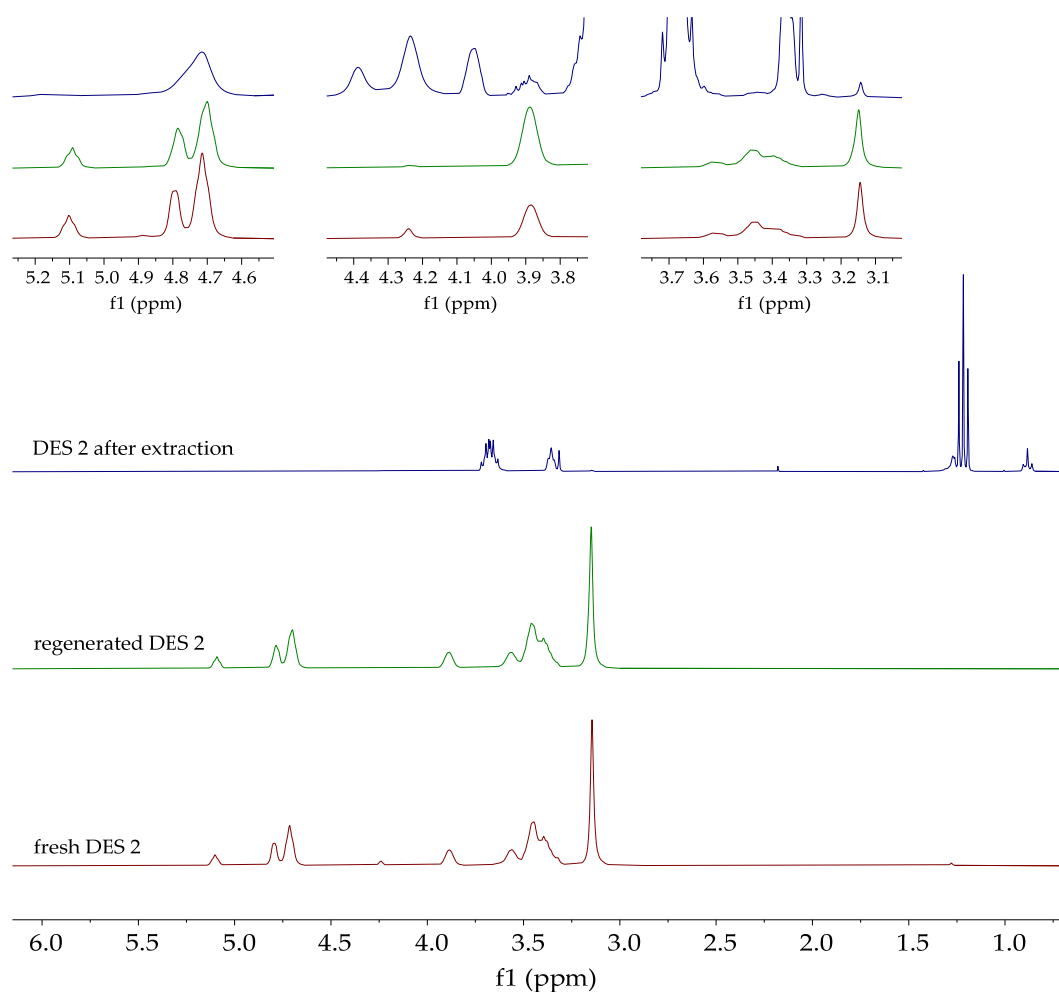


Figure 4. ^1H NMR spectra of DES 2: after extraction, regenerated and freshly prepared.

4. Conclusions

The research described in this article compared the efficiencies of several different separation techniques, namely liquid–liquid extraction, extractive distillation aided with several DESs, non-entrained distillation as well as reduced pressure distillation for separating the azeotropic mixture of *n*-hexane and ethanol.

The two menthol-based hydrophobic DESs were tested as entrainers for extractive distillation. Both of them were shown to enhance the separation of *n*-hexane from ethanol, and the method outperformed reduced pressure distillation. The hydrophilic choline chloride-based DES 2 as entrainer did increase the *n*-hexane distillate content compared to atmospheric distillation, but it did not match the efficiency of hydrophobic DESs or reduced pressure distillation.

Experimental liquid–liquid equilibrium data in the system involving DES 2 were described with the NRTL and UNIQUAC activity coefficient models. The latter one exhibited superior accuracy as proven by the smaller root mean square deviation value and thus may be suggested as a more reliable tool in modeling similar separation processes.

The study explored the effect of varying DES-to-feed mass ratios on extraction efficiency; the higher ratios always resulted in better performance. In addition, the successful regeneration of DES 2 via evaporation of *n*-hexane and ethanol, verified by NMR spectroscopy, emphasized the reusability of the DES.

The possible use of hydrophobic DESs in industrial extraction applications is yet to be tested, in particular in terms of their long-term stability and environmental impact. Further research into other hydrophilic and hydrophobic DES combinations could also unveil new opportunities for the optimization of separation processes.

Author Contributions: Conceptualization, A.S. and A.P.; methodology, A.S., A.P., M.R. and M.C.; software, A.S., A.P. and M.R.; formal analysis, A.S., A.P. and M.C.; investigation, A.S., A.P., M.Ž. and L.F.; resources, A.S.; data curation, A.S., A.P. and M.R.; writing—original draft preparation, A.S., A.P. and M.R.; writing—review and editing, A.S., A.P. and M.R.; visualization, A.S. and A.P.; supervision, A.S. All authors have read and agreed to the published version of the manuscript.

Funding: This research received no external funding.

Data Availability Statement: The original contributions presented in the study are included in the article, further inquiries can be directed to the corresponding authors.

Acknowledgments: The authors acknowledge the use of AI, specifically ChatGPT, for language editing purposes.

Conflicts of Interest: The authors declare no conflicts of interest.

References

1. Oliveira, F.S.; Pereiro, A.B.; Rebelo, L.P.N.; Marrucho, I.M. Deep Eutectic Solvents as Extraction Media for Azeotropic Mixtures. *Green Chem.* **2013**, *15*, 1326–1330. [[CrossRef](#)]
2. Gouveia, A.S.L.; Oliveira, F.S.; Kurnia, K.A.; Marrucho, I.M. Deep Eutectic Solvents as Azeotrope Breakers: Liquid-Liquid Extraction and COSMO-RS Prediction. *ACS Sustain. Chem. Eng.* **2016**, *4*, 5640–5650. [[CrossRef](#)]
3. Sharepour, F.; Bakhshi, H.; Rahimnejad, M. Separation of Ethanol Azeotropic Mixture Using Deep Eutectic Solvents in Liquid-Liquid Extraction Process. *J. Mol. Liq.* **2021**, *338*, 116637. [[CrossRef](#)]
4. Sa, E.J.; Lee, B.S.; Park, B.H. Extraction of Ethanol from Mixtures with N-Hexane by Deep Eutectic Solvents of Choline Chloride + Levulinic Acid, + Ethylene Glycol, or + Malonic Acid. *J. Mol. Liq.* **2020**, *316*, 113877. [[CrossRef](#)]
5. Vuksanović, J.; Kijevčanin, M.L.; Radović, I.R. Effect of Water Addition on Extraction Ability of Eutectic Solvent Choline Chloride+ 1,2-Propanediol for Separation of Hexane/Heptane+ethanol Systems. *Korean J. Chem. Eng.* **2018**, *35*, 1477–1487. [[CrossRef](#)]
6. Domańska, U.; Zołek-Tryznowska, Z.; Pobudkowska, A. Separation of Hexane/Ethanol Mixtures. LLE of Ternary Systems (Ionic Liquid or Hyperbranched Polymer + Ethanol + Hexane) at T = 298.15 K. *J. Chem. Eng. Data* **2009**, *54*, 972–976. [[CrossRef](#)]
7. Ma, Y.; Xu, X.; Wen, G.; Xu, D.; Shi, P.; Wang, Y.; Gao, J. Separation of Azeotropes Hexane + Ethanol/1-Propanol by Ionic Liquid Extraction: Liquid-Liquid Phase Equilibrium Measurements and Thermodynamic Modeling. *J. Chem. Eng. Data* **2017**, *62*, 4296–4300. [[CrossRef](#)]
8. Rodriguez, N.R.; Molina, B.S.; Kroon, M.C. Aliphatic+ethanol Separation via Liquid-Liquid Extraction Using Low Transition Temperature Mixtures as Extracting Agents. *Fluid. Phase Equilib.* **2015**, *394*, 71–82. [[CrossRef](#)]

9. Samarov, A.A.; Smirnov, M.A.; Sokolova, M.P.; Popova, E.N.; Toikka, A.M. Choline Chloride Based Deep Eutectic Solvents as Extraction Media for Separation of N-Hexane–Ethanol Mixture. *Fluid. Phase Equilib.* **2017**, *448*, 123–127. [CrossRef]
10. Cai, F.; Zhao, M.; Wang, Y.; Wang, F.; Xiao, G. Phosphoric-Based Ionic Liquids as Solvents to Separate the Azeotropic Mixture of Ethanol and Hexane. *J. Chem. Thermodyn.* **2015**, *81*, 177–183. [CrossRef]
11. Medina-Herrera, N.; Grossmann, I.E.; Mannan, M.S.; Jiménez-Gutiérrez, A. An Approach for Solvent Selection in Extractive Distillation Systems Including Safety Considerations. *Ind. Eng. Chem. Res.* **2014**, *53*, 12023–12031. [CrossRef]
12. Chen, Y.; Wu, Q.; Wang, Y.; Sun, C.; Xue, K.; Guo, C.; Zhu, Z.; Wang, Y.; Cui, P. Phase Equilibria and Mechanism Analysis of Separating Ethanol from Fuel Additives by Chord Chloride-Deep Electrochemical Solvents. *J. Mol. Liq.* **2023**, *392*, 123434. [CrossRef]
13. Petračić, A.; Sander, A.; Vuković, J.P. Deep Eutectic Solvents for Deacidification of Waste Biodiesel Feedstocks: An Experimental Study. *Biomass Convers. Biorefin* **2021**, *11*, 3–23. [CrossRef]
14. Sander, A.; Petračić, A.; Vrsaljko, D.; Parlov Vuković, J.; Hršak, P.; Jelavić, A. Continuous Purification of Biodiesel with Deep Eutectic Solvent in a Laboratory Karr Column. *Separations* **2024**, *11*, 71. [CrossRef]
15. Rogošić, M.; Sander, A.; Pantaler, M. Application of 1-Pentyl-3-Methylimidazolium Bis(Trifluoromethylsulfonyl) Imide for Desulfurization, Denitrification and Dearomatization of FCC Gasoline. *J. Chem. Thermodyn.* **2014**, *76*, 1–15. [CrossRef]
16. Al-Risheq, D.I.M.; Nasser, M.S.; Qiblawey, H.; Ba-Abbad, M.M.; Benamor, A.; Hussein, I.A. Destabilization of Stable Bentonite Colloidal Suspension Using Choline Chloride Based Deep Eutectic Solvent: Optimization Study. *J. Water Process. Eng.* **2021**, *40*, 101885. [CrossRef]
17. Mulia, K.; Krisanti, E.; Terahadi, F.; Putri, S. Selected Natural Deep Eutectic Solvents for the Extraction of α -Mangostin from Mangosteen (*Garcinia mangostana* L.) Pericarp. *Int. J. Technol.* **2015**, *6*, 1211–1220. [CrossRef]
18. Haghbakhsh, R.; Raeissi, S. A Study of Non-Ideal Mixtures of Ethanol and the (1 Choline Chloride +2 Ethylene Glycol) Deep Eutectic Solvent for Their Volumetric Behaviour. *J. Chem. Thermodyn.* **2020**, *150*, 106219. [CrossRef]
19. Petris, P.C.; Anogiannakis, S.D.; Tzounis, P.-N.; Theodorou, D.N. Thermodynamic Analysis of *n*-Hexane–Ethanol Binary Mixtures Using the Kirkwood–Buff Theory. *J. Phys. Chem. B* **2019**, *123*, 247–257. [CrossRef]
20. Jukić, I.; Požar, M.; Lovrinčević, B. Comparative Analysis of Ethanol Dynamics in Aqueous and Non-Aqueous Solutions. *Phys. Chem. Chem. Phys.* **2020**, *22*, 23856–23868. [CrossRef]
21. Published Parameters UNIFAC—DDBST GmbH. Available online: <https://www.ddbst.com/published-parameters-unifac.html> (accessed on 10 May 2024).
22. Renon, H.; Prausnitz, J.M. Local Compositions in Thermodynamic Excess Functions for Liquid Mixtures. *AIChE J.* **1968**, *14*, 135–144. [CrossRef]
23. Abrams, D.S.; Prausnitz, J.M. Statistical Thermodynamics of Liquid Mixtures: A New Expression for the Excess Gibbs Energy of Partly or Completely Miscible Systems. *AIChE J.* **1975**, *21*, 116–128. [CrossRef]
24. Magnussen, T.; Rasmussen, P.; Fredenslund, A. UNIFAC Parameter Table for Prediction of Liquid-Liquid Equilibria. *Ind. Eng. Chem. Process. Des. Dev.* **1981**, *20*, 331–339. [CrossRef]
25. Rogošić, M.; Zagajski Kučan, K. Modelling of Liquid–Liquid Equilibria in Quasi-Seven-Component Systems with Deep Eutectic Solvents as Extraction Media. *Kem. Ind.* **2018**, *67*, 385–402. [CrossRef]
26. Casal, M.F. Desulfurization of Fuel Oils by Solvent Extraction with Ionic Liquids. PhD Thesis, University of Santiago de Compostela, Santiago de Compostela, Spain, 2010.
27. Marcilla, A.; Reyes-Labarta, J.A.; Olaya, M.M. Should We Trust All the Published LLE Correlation Parameters in Phase Equilibria? Necessity of Their Assessment Prior to Publication. *Fluid. Phase Equilib.* **2017**, *433*, 243–252. [CrossRef]
28. Sa, E.J.; Lee, B.S.; Park, B.H. Separation of N-Hexane-Ethanol Azeotropic Mixture Using Choline Chloride +1,4-Butanediol Deep Eutectic Solvents. *Chem. Eng. Res. Des.* **2023**, *192*, 1–11. [CrossRef]

Disclaimer/Publisher’s Note: The statements, opinions and data contained in all publications are solely those of the individual author(s) and contributor(s) and not of MDPI and/or the editor(s). MDPI and/or the editor(s) disclaim responsibility for any injury to people or property resulting from any ideas, methods, instructions or products referred to in the content.